Four-band model for oxygen holes in copper oxide superconductors. I. Quasiparticles

Lior Klein and Amnon Aharony
School of Physics and Astronomy, Beverly and Raymond Sackler Faculty of Exact Sciences, Tel Aviv University, Tel Aviv 69978, Israel
(Received 22 May 1991)

All the high-temperature superconductors have copper oxide planes with strong antiferromagnetic correlations. In many of these, the charge is carried by quasiparticles which are based on holes that move on the oxygen ions. We study the effect of the antiferromagnetic background of the Cu spins in the CuO_2 planes on the spectrum of the mobile quasiparticles. We consider several possible quasiparticles, which involve the spin of the hole and the spins of the two neighboring copper ions. For each quasiparticle we obtain, using tight-binding methods, four energy bands. We find that the favored charge carrier is a spin $\frac{1}{2}$ quasiparticle. The minimum of the lowest energy band is at the points $\mathbf{k}=(0,\pm\pi/2\bar{a})$ and $\mathbf{k}=(\pm\pi/2\bar{a},0)$, where the x and y directions are along the nearest-neighbors oxygen-oxygen bonds (of length $\bar{a}$) in the CuO_2 plane. The effective mass is less than $3.7m_e$, in good agreement with measurements of the London penetration depth for $La_{2-x}Sr_xCuO_4$. It is also consistent with these measurements for the Bi and Tl compounds. However, we obtain conflicting results for $YBa_2Cu_3O_{6+y}$, possibly due to the fact that the CuO chains also superconduct.

I. INTRODUCTION

CuO_2 planes are a common ingredient in many high-temperature superconductors (HTSC): $La_{2-x}Sr_xCuO_4$,[1] $YBa_2Cu_3O_{6+y}$,[2] $Tl_2Ba_2Ca_{m-1}Cu_mO_{2m+4}$,[3] and many others. Therefore, it is commonly believed that the study of these planes will help us reveal the properties of the HTSC. In pure La_2CuO_4 or $YBa_2Cu_3O_6$, for instance, the CuO_2 planes cannot be candidates for being building bricks of a superconductor, since they are Mott insulators.[4] They conduct only when the doping of La_2CuO_4 with Sr or the doping of $YBa_2Cu_3O_6$ with oxygen exceeds some critical threshold. Therefore, one should figure out the electronic structure of the perfect planes as well as the nature of the holes, generated upon doping.

The electronic structure of the planes was the focus of intensive experimental effort using various techniques, including high-energy spectroscopy such as electron-energy-loss spectroscopy in transmission,[5] x-ray photoemission spectroscopy,[6] x-ray absorption spectroscopy,[7] and nuclear magnetic resonance.[8] The overall conclusions of these experiments and many others were: (a) the Cu (in the undoped CuO_2 planes) is in a Cu^{2+} state with a hole in the $d_{x^2-y^2}$ orbital. (b) The doped holes are dominantly oxygen holes. (c) There is evidence that the doped hole is probably in the antibonding p_σ orbital of the oxygen, hybridized with the Cu-$d_{x^2-y^2}$ state, but the possibility that it is in the nonbinding p_π orbital hybridized with the Cu-d_{xy} state is not ruled out.[5,9,10]

These compounds also exhibit interesting magnetic features. The Cu in the CuO_2 planes has a localized spin-$\frac{1}{2}$ hole and there is an antiferromagnetic (AFM) coupling J between neighboring Cu spins and also a weak coupling between adjacent CuO_2 layers. These induce a three dimensional Néel transition in the undoped case.[11] Upon doping we generate spin-$\frac{1}{2}$ holes on the oxygen sites. The oxygen spin has an exchange interaction J_σ with the two nearest-neighbor Cu's. The Cu-oxygen distance is half the Cu-Cu distance, therefore $|J_\sigma| \gg |J|$, thus introducing an effective ferromagnetic interaction between the two Cu neighbors of the oxygen hole. This was the basic idea of the frustration model of Aharony and co-workers.[12] This model correctly predicted the existence of a spin-glass state, which was simultaneously detected experimentally.[13–16]

The doping rapidly decreases the Néel temperature until the disappearance of the long-range AFM order. Nevertheless, AFM spin correlations in the CuO_2 plane of order 10–20 Å were detected by neutron scattering[17] and nuclear quadrupole resonance,[18] in the metallic and in the superconducting phases of $La_{2-x}Sr_xCuO_4$. Therefore, AFM correlations are present and may play an important role in the superconducting phase. One should notice that AFM order is not a pair breaker,[19] thus there is a possibility of coexistence of AFM order and superconductivity.

Many theoretical models were implemented in handling the CuO_2 planes in the HTSC. These include (a) a one-band tight binding model,[20] (b) a one-band Hubbard model[21] for a complex local singlet quasiparticle consisting of a Cu hole and a hole shared by its four oxygen neighbors, (c) a three-band Hubbard model, where the mobile holes can be on the Cu or on the oxygen sites,[22] (d) a Hamiltonian that combines Heisenberg exchange and the kinetic energy of the mobile holes, so called t-J one-band model,[23] and (e) a two-band model in which enhanced pairing interaction is obtained.[24]

The structure of the CuO_2 planes in the paramagnetic and in the AFM phases is shown in Figs. 1(a) and 1(b). In the undoped case we have Cu^{2+} and O^{2-}. Doping introduces holes on some oxygen sites, which become O^-.

These additional holes hop between oxygen sites and there is also a strong exchange interaction between the spin of the oxygen hole and the spins of its two Cu neighbors.

Emery and Reiter[25] (ER) presented for this system an effective Hamiltonian derived from a three-band Hubbard model,

$$H_{\text{eff}}=(t_1+t_2)\sum_{\Delta\neq\Delta',m,\sigma,\sigma'} a^{\dagger}_{m\sigma'}a_{m\sigma}a^{\dagger}_{m+\Delta,\sigma}a_{m+\Delta',\sigma'} -t_2\sum_{\Delta\neq\Delta',m,\sigma} a^{\dagger}_{m+\Delta,\sigma}a_{m+\Delta',\sigma} +J_{\sigma}\sum_{m,\Delta}(\mathbf{S}_m\cdot\mathbf{S}_{m+\Delta}-\tfrac{1}{4})n_{m+\Delta}\ , \tag{1.1}$$

where $a(a^{\dagger})$ is the annihilation (creation) fermionic operator, m indicates the Cu sites, and $m+\Delta$ the neighboring oxygen sites. σ indicates a spin index. $\mathbf{S}$ is a Heisenberg spin operator.

A process of an oxygen hole hopping between two oxygen sites, which involves a spin flip of the hole, may be induced only by the first part of the Hamiltonian. Such a hopping without a spin flip may be induced by the two first terms of the Hamiltonian. The amplitudes for these two processes are therefore, t_1+t_2 and t_1, respectively. This effective Hamiltonian contains only hops of oxygen holes through the Cu sites; direct hops between nearest-neighbor oxygen sites were neglected. However, numerical calculations[10,26–29] show that we should take into account these direct hops. Thus we add to the effective Hamiltonian another term, which distinguishes between hops from site 1 to site 2 and hops from site 1 to site 4 in Fig. 1(b),

$$t_0\sum_{\Delta\neq\Delta',m,\sigma}\omega(\Delta,\Delta')a^{\dagger}_{m+\Delta,\sigma}a_{m+\Delta',\sigma}\ , \tag{1.2}$$

where $t_0=t_{pp}$ (t_{pp} is the overlap integral of two oxygen holes that are nearest neighbors, e.g., sites 1 and 2 in Fig. 1), and where $\omega(\Delta,\Delta')=1$ when $m+\Delta$ and $m+\Delta'$ are sites of two nearest-neighbor oxygens [e.g., sites 1 and 2 in Fig. 1(b)] and $\omega(\Delta,\Delta')=0$, otherwise.

The values that were calculated numerically by a variety of methods are: the onsite energies of a hole on the oxygen (ε_p) or on the Cu (ε_d), with $\varepsilon=\varepsilon_p-\varepsilon_d$, the onsite Coulomb repulsion between two holes on a Cu site (U_d), the Coulomb repulsion between Cu-O neighboring holes (V), and the hopping integral between Cu-O neighbors (t). The parameters t_1 and t_2, which appear in the effective Hamiltonian, are determined by the use of perturbation theory, and we quote[25]

$$t_1=\frac{1}{2}\left|\frac{\varepsilon}{2}-\left[\left[\frac{\varepsilon}{2}\right]^2+2t^2\right]^{0.5}\right|\ , \qquad t_2=\frac{t^2}{U_d-2V-\varepsilon}\ . \tag{1.3}$$

In our case $t/(U_d-2V-\varepsilon)\ll 1$, and therefore the regular perturbation theory is sufficient for determining t_2. However, t/ε is of order one, thus the convergence of the regular perturbation series is not fast enough. To overcome this difficulty, ER used the Winger-Brillouin perturbation theory to evaluate t_1.

In Table I we present some of these calculated parameters. The Cu-O hopping integral t depends on the symmetry of the oxygen hole. When the hole occupies a p orbital, which is directed in the Cu-O direction (a so-called σ state), we denote t as $t_{pd\sigma}$ and the band (so-called $p\sigma$ band) consists of oxygen p orbitals hybridized with Cu-$d_{x^2-y^2}$ orbitals. When the hole occupies a p orbital, which is directed perpendicular to the Cu-O direction (a so-called π state) we denote t as $t_{pd\pi}$ and the band (a so-called $p\pi$ band) consists of oxygen p orbitals hybridized with Cu-d_{xy} orbitals. The parameters $t_{pp\sigma}$ and $t_{pp\pi}$ are the direct hopping amplitudes between two nearest-neighbor oxygens when the hole occupies a σ or π state, respectively. As can be seen from Table I, there are some differences between different numerical estimates of the effective parameters. For the $p\sigma$ band we chose to use $t_1=0.43$ eV and $t_2=0.22$ eV, as suggested by ER.[25] There is an ambiguity concerning the sign of t_0. Frenkel *et al.*[29] argue that it should be negative, $t_0=-0.7$ eV. We accept this claim but, since the more common value is $|t_0|=0.65$ eV,[10,26,28] we use $t_0=-0.65$ eV. For a $p\pi$ band we use the relation $t_{pd\pi}\sim -0.5t_{pd\sigma}$ (Refs. 27 and 28) to obtain $t_1=0.14$ eV and $t_2=0.055$ eV (also using the ER set of parameters). Stechel and Jennison[27] found that $t_{pp\pi}=t_{pp\sigma}$ (indeed one can see that disregarding the Cu effect on the oxygen orbitals, the overlap integral is the

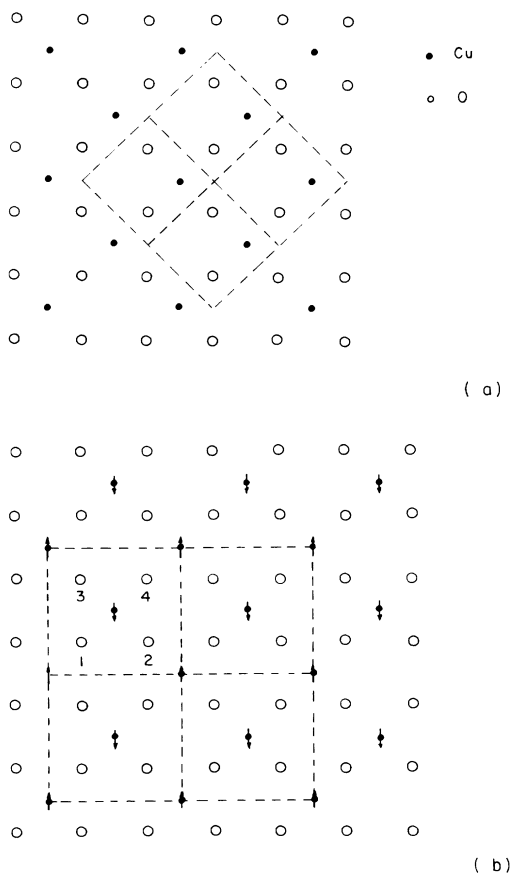

FIG. 1. Nonmagnetic 1(a) and magnetic 1(b) unit cells.

TABLE I. Comparison of the parameters that different authors use in the Hubbard model.

	Ref. 25	Ref. 27	Ref. 29	Ref. 28	Ref. 26	Ref. 10	Our choice
ε	1.5	1.5	1.5	3.5	3.6	1.2	1.5
$t_{pd\sigma}$	1	1.07	1.4	1.3	1.3	−1.6	1
$t_{pp\sigma}$		0.53	−0.7	0.65	0.65	0.65	−0.65
$t_{pp\pi}$		0.53					−0.65
U_d	9	9	9	8.8	10.5	8.5	9
U_p	6	6	6	6	4	4.1–7.3	6
V	1.5	1.5	1.6		1.2	0.6–1.3	1.5
t_1	0.43	0.47	0.68		0.39		0.43
t_2	0.22	0.25	0.46		0.37		0.22

same in both cases). Therefore, for consistency, we use $t_{pp\pi}=-0.65$ eV.

In this paper we handle the CuO_2 plane by using the following simplifying assumptions: (a) The charge carrier [the quasiparticle] is an eigenstate of the exchange interaction part, i.e., the last term in Eq. (1.1). (b) The Cu spins are in a Néel state (at low enough temperature) even in the superconducting phase. (c) The movement of the quasiparticle does not disturb the Néel state of the Cu spins.

Assumption (a) was introduced by Aharony and coworkers[12] and it is reasonable, since the spin of the doped oxygen hole is strongly coupled to the spins of its two Cu neighbors. Thus, we may consider these strongly coupled three spins as the relevant moving quasiparticle in our system.

We are aware that experiments do not indicate the existence of a Néel state in the superconducting phase [as assumed in (b)], but rather find finite range AFM correlations. Nevertheless, AFM order can, in principle, coexist with superconductivity. Since there exist AFM correlations, the hole "sees" an AFM background and this approximation may not be too bad. The nonmagnetic unit cell of the CuO_2 plane [Fig. 1(a)] consists of one Cu and two oxygens. However, the magnetic unit cell [Fig. 1(b)] consists of two Cu's and four oxygens. *A priori,* we would have six bands (two coppers and four oxygens). Assuming that the holes move only on the oxygens, reduces the number of bands to four.

When the quasiparticles move on the AFM background they naturally disturb the AFM order. However, this disturbance makes the calculation of the bands very complicated and actually brings us back to the *t-J* model, which cannot be solved exactly. For the sake of having simple analytic results we have decided to lose some of the accuracy by considering only quasiparticle hops that do not disturb the AFM background. This implies that the effective mass of the quasiparticles, which is calculated under such constraints, is an overestimate.

Our plan is to identify the quasiparticles that are eigenstates of the exchange part in the effective Hamiltonian. Then we determine the hopping amplitudes of the quasiparticles. We use these amplitudes in a tight binding model. Since we assume that the Cu spins are in a Néel state, the unit cell consists of four oxygens, thus leading to a four-band model. We choose the best quasiparticle and the lowest energy band. We then calculate the in-plane effective mass, and compare the results with measurements of the London penetration depth in several materials.

The remainder of this paper is organized as follows. In Sec. II, we study the nature of the quasiparticle. In Sec. III, we obtain the parameters of the tight-binding model for the various quasiparticle. In Sec. IV, we obtain the four tight-binding bands. In Sec. V, we use the lowest energy band to calculate the effective mass and the London penetration depths and Sec. VI contains our summary and discussion.

II. THE QUASIPARTICLES

The excess mobile holes in the CuO_2 planes reside mainly on the oxygen ions. Each hole is strongly coupled to its two neighboring Cu's holes and the relevant Hamiltonian [which is the exchange term in Eq. (1.1)] is[12]

$$H_{\rm ex}=-J_\sigma(\mathbf{S}_1+\mathbf{S}_3)\cdot\mathbf{S}_2 , \tag{2.1}$$

where $\mathbf{S}_2$ is the oxygen spin and $\mathbf{S}_1$ and $\mathbf{S}_3$ are the neighboring Cu's spins.

Since the overlap integral that determines the strength of the exchange interaction decreases exponentially with the distance between the spins, we would expect that $|J_\sigma| \gg |J|$, where J is the exchange between the neighboring Cu's in the undoped case (Frenkel *et al.*,[29] for instance, estimated $J\simeq -0.13$ eV and $J_\sigma \simeq -0.36$ eV, when the oxygen hole is assumed to be in a σ state). Indeed, Monte Carlo simulations[30] confirmed that the doped holes on oxygen sites couple strongly with the neighboring Cu spins. Thus it is reasonable to regard the spin eigenstates of $H_{\rm ex}$ as the relevant mobile quasiparticles. Once the quasiparticles are determined and fixed we can drop $H_{\rm ex}$ from the effective Hamiltonian. The idea that the charge carrier is a complex particle of this sort received different names, like spin polaron,[25] spin hybrid,[27] and spin bag.[31] Nevertheless, we believe that the basic physics is common.

We can easily find the eigenstates of $H_{\rm ex}$ by diagonalizing its 8×8 matrix in the basis of the three spin states, (S_{1z}, S_{2z}, S_{3z}). This matrix has three eigenvalues $-0.5J_\sigma$, J_σ, and 0. Notice that we can rewrite Eq. (2.1) in the form[12]

$$H_{\rm ex}=-J_\sigma(S^2-S_{13}^2-S_2^2)/2 , \tag{2.2}$$

where

$$\mathbf{S}=\mathbf{S}_1+\mathbf{S}_2+\mathbf{S}_3$$

and

$$\mathbf{S}_{13}=\mathbf{S}_1+\mathbf{S}_3 .$$

Since H_{ex} commutes with S^2, S_{13}^2, and S_z, its eigenstates may be classified according to the eigenvalues of S^2 and S_{13}^2, which are $s(s+1)$ and $s_{13}(s_{13}+1)$, respectively, and of S_z, which has the $2s+1$ eigenvalues s, $s-1$, $s-2,\ldots,-s$. The eigenvalues of H_{ex} are given by

$$-0.5J_\sigma[s(s+1)-s_{13}(s_{13}+1)-\tfrac{3}{4}] .$$

There are four eigenstates $|\alpha_i\rangle$ with the energy eigenvalue $-0.5J_\sigma$, $s=\frac{3}{2}$, and $s_{13}=1$:

$$\begin{aligned}
|\alpha_1\rangle&=|\uparrow\uparrow\uparrow\rangle ,\\
|\alpha_2\rangle&=\frac{1}{\sqrt{3}}(|\downarrow\uparrow\uparrow\rangle+|\uparrow\downarrow\uparrow\rangle+|\uparrow\uparrow\downarrow\rangle) ,\\
|\alpha_3\rangle&=\frac{1}{\sqrt{3}}(|\uparrow\downarrow\downarrow\rangle+|\downarrow\uparrow\downarrow\rangle+|\downarrow\downarrow\uparrow\rangle) ,\\
|\alpha_4\rangle&=|\downarrow\downarrow\downarrow\rangle .
\end{aligned} \tag{2.3}$$

There are two eigenstates $|\beta_i\rangle$ with the eigenvalue J_σ, $s=\frac{1}{2}$, and $s_{13}=1$:

$$\begin{aligned}
|\beta_1\rangle&=\frac{1}{\sqrt{6}}[2|\uparrow\downarrow\uparrow\rangle-(|\downarrow\uparrow\uparrow\rangle+|\uparrow\uparrow\downarrow\rangle)] ,\\
|\beta_2\rangle&=\frac{1}{\sqrt{6}}[2|\downarrow\uparrow\downarrow\rangle-(|\uparrow\downarrow\downarrow\rangle+|\downarrow\downarrow\uparrow\rangle)] .
\end{aligned} \tag{2.4}$$

Both cases of $s_{13}=1$ imply a strong ferromagnetic correlation between $\mathbf{S}_1$ and $\mathbf{S}_3$. Since this competes with the AFM order, it causes the emergence of a spin-glass phase,[12] when the quasiparticle is localized.

There are also two states,

$$|\gamma_1\rangle=(1/\sqrt{2})(|\uparrow\uparrow\downarrow\rangle-|\downarrow\uparrow\uparrow\rangle)$$

and

$$|\gamma_2\rangle=(1/\sqrt{2})(|\downarrow\downarrow\uparrow\rangle-|\uparrow\downarrow\downarrow\rangle) ,$$

with energy eigenvalue 0, which correspond to $s=\frac{1}{2}$ and $s_{13}=0$. However, these states are never the groundstate. The sign of J_σ determines which of the other two sets of eigenstates is favorable. This sign depends on the orbital of the doped hole. Hund's rules, as well as numerical calculations (e.g., Ref. 28) have demonstrated that if the doped hole is in the antibonding σ state (nonbinding π) then $J_\sigma<0$ ($J_\sigma>0$). These calculations also seem to favor the σ-state option, which implies that $J_\sigma<0$. However, photoemission studies, which probe the hole symmetry[32] cannot differentiate between σ holes or in-plane π holes. Therefore, *a priori*, we cannot rule out the π-holes option. From now on we call the eigenstates with eigenvalue $-0.5J_\sigma$, spin-$\frac{3}{2}$ states and those with eigenvalue J_σ, spin-$\frac{1}{2}$ states.

We expect the best quasiparticle to be a superposition of spin-$\frac{1}{2}$ eigenstates or of spin-$\frac{3}{2}$ eigenstates. Consider first the spin-$\frac{1}{2}$ case. Assuming that the spin of the quasiparticle points along the z direction (chosen to be the direction of the Cu AFM staggered magnetization), then the quasiparticle state would be

$$|\mathrm{qp}\rangle_1=|\beta_1\rangle=\frac{1}{\sqrt{6}}[2|\uparrow\downarrow\uparrow\rangle-(|\downarrow\uparrow\uparrow\rangle+|\uparrow\uparrow\downarrow\rangle)] . \tag{2.5a}$$

If, on the other hand, the spin of the quasiparticle is orthogonal to the z axis, then a representative state of the quasiparticle would be

$$|\mathrm{qp}\rangle_2=\frac{1}{\sqrt{2}}(|\beta_1\rangle+|\beta_2\rangle)=\frac{1}{\sqrt{12}}[2|\uparrow\downarrow\uparrow\rangle-(|\downarrow\uparrow\uparrow\rangle+|\uparrow\uparrow\downarrow\rangle)+2|\downarrow\uparrow\downarrow\rangle-(|\uparrow\downarrow\downarrow\rangle+|\downarrow\downarrow\uparrow\rangle)] , \tag{2.5b}$$

where the quasiparticle spin points along the x axis.

For the spin-$\frac{3}{2}$ case, we similarly consider the following quasiparticles

$$|\mathrm{qp}\rangle_3=|\alpha_2\rangle=\frac{1}{\sqrt{3}}(|\downarrow\uparrow\uparrow\rangle+|\uparrow\downarrow\uparrow\rangle+|\uparrow\uparrow\downarrow\rangle) , \tag{2.6a}$$

$$|\mathrm{qp}\rangle_4=\frac{1}{\sqrt{2}}(|\alpha_2\rangle+|\alpha_3\rangle)=\frac{1}{\sqrt{6}}(|\downarrow\uparrow\uparrow\rangle+|\uparrow\downarrow\uparrow\rangle+|\uparrow\uparrow\downarrow\rangle+|\uparrow\downarrow\downarrow\rangle+|\downarrow\uparrow\downarrow\rangle+|\downarrow\downarrow\uparrow\rangle) , \tag{2.6b}$$

$$|\mathrm{qp}\rangle_5=|\alpha_1\rangle=|\uparrow\uparrow\uparrow\rangle . \tag{2.6c}$$

III. TIGHT-BINDING PARAMETERS

Having diagonalized the last term in Eq. (1.1), we now derive the tight-binding Hamiltonian, which describes the hops of the quasiparticles between the oxygen sites. We start with the effective Hamiltonian

$$H_{\mathrm{eff}}=(t_1+t_2)\sum_{\Delta\neq\Delta',m,\sigma,\sigma'} a^\dagger_{m\sigma'}a_{m\sigma}a^\dagger_{m+\Delta,\sigma}a_{m+\Delta',\sigma'}-t_2\sum_{\Delta\neq\Delta',m,\sigma} a^\dagger_{m+\Delta,\sigma}a_{m+\Delta',\sigma}+t_0\sum_{\Delta\neq\Delta',m,\sigma}\omega(\Delta,\Delta')a^\dagger_{m+\Delta,\sigma}a_{m+\Delta',\sigma} . \tag{3.1}$$

We consider two cases. In the first case (which is more probable) the hole is in a σ state; the effective parameters are $t_1=0.43$ eV, $t_2=0.22$ eV, and $|\mathrm{qp}\rangle_1$ and $|\mathrm{qp}\rangle_2$ have the lowest exchange energy ($J_\sigma<0$). In the second case the hole is in a π state; $t_1=0.14$ eV, $t_2=0.055$ eV, and $|\mathrm{qp}\rangle_3$, $|\mathrm{qp}\rangle_4$, and $|\mathrm{qp}\rangle_5$ have the lowest exchange energy ($J_\sigma>0$). In both

cases we use $t_0=-0.65$ eV.

Let us examine Fig. 2. Five sites participate in a hopping of a quasiparticle: (1), (3), and (5) are Cu sites and (2) and (4) are oxygen sites. The quasiparticle is initially in sites (1), (2), and (3), and it hops to sites (3), (4), and (5) [see Figs. 2(a) and 2(b)]. Before the hopping, the z component of the spin at site (5) is equal to σ, determined by the Néel ordering ($\sigma=\downarrow$ in the example of Fig. 2). Since sites (1) and (5) belong to the same AFM sublattice we assume that after the hopping the z component of the spin at site (1) is also equal to σ. Initially, the five spins are in the state $|\psi_\sigma\rangle\equiv|(\mathrm{qp})0\sigma\rangle$, where (qp) denotes one of the quasiparticle states discussed above, the "0" denotes an "empty" oxygen site and σ denotes the spin of site (5). For example, for $|\mathrm{qp}\rangle_5$ we have $|\psi_\sigma\rangle=|\uparrow\uparrow\uparrow 0\sigma\rangle$. The final state is similarly written as $|\psi'_\sigma\rangle\equiv|\sigma 0(\mathrm{qp})'\rangle$.

For a spin-$\frac{3}{2}$ quasiparticle, we use

$$|\mathrm{qp}\rangle=\sum_{i=1}^{4}c_i|\alpha_i\rangle,\quad |\mathrm{qp}\rangle'=\sum_{i=1}^{4}c'_i|\alpha_i\rangle \tag{3.2}$$

and find

$$\langle\psi_\uparrow|H_{\mathrm{eff}}|\psi'_\uparrow\rangle=(c_1^*c'_1+\tfrac{2}{3}c_2^*c'_2+\tfrac{1}{3}c_3^*c'_3)[t_1+t_0\omega(\Delta,\Delta')] \tag{3.3}$$

and

$$\langle\psi_\downarrow|H_{\mathrm{eff}}|\psi'_\downarrow\rangle=(c_4^*c'_4+\tfrac{2}{3}c_3^*c'_3+\tfrac{1}{3}c_2^*c'_2)[t_1+t_0\omega(\Delta,\Delta')]\ . \tag{3.4}$$

Similarly for a spin-$\frac{1}{2}$ quasiparticle we use

$$|\mathrm{qp}\rangle=\sum_{i=1}^{2}d_i|\beta_i\rangle,\quad |\mathrm{qp}\rangle'=\sum_{i=1}^{2}d'_1|\beta_i\rangle\ , \tag{3.5}$$

and thus

$$\langle\psi_\uparrow|H_{\mathrm{eff}}|\psi'_\uparrow\rangle=(t_1+t_2)(-\tfrac{2}{3}d_1^*d'_1+\tfrac{1}{6}d_2^*d'_2)+[-t_2+t_0\omega(\Delta,\Delta')](\tfrac{5}{6}d_1^*d'_1+\tfrac{1}{6}d_2^*d'_2) \tag{3.6}$$

and

$$\langle\psi_\downarrow|H_{\mathrm{eff}}|\psi'_\downarrow\rangle=(t_1+t_2)(-\tfrac{2}{3}d_2^*d'_2+\tfrac{1}{6}d_1^*d'_1)+[-t_2+t_0\omega(\Delta,\Delta')](\tfrac{5}{6}d_2^*d'_2+\tfrac{1}{6}d_1^*d'_1)\ . \tag{3.7}$$

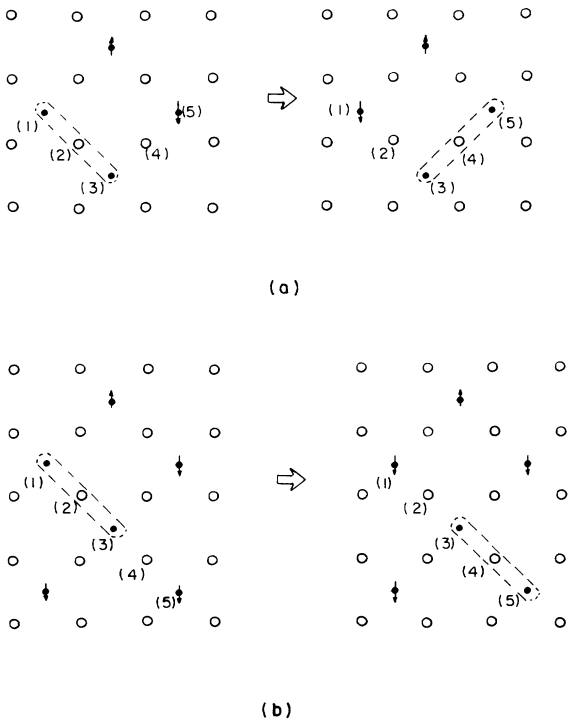

FIG. 2. Two possible hops of a quasiparticle.

The explicit dependence on σ represents the dependence of the hopping of the quasiparticle on the magnetic background. Therefore, a tight-binding model will consist of four oxygen sites in each unit cell. In Fig. 3 we show the unit cell and the four hopping amplitudes, t_a,t_b,t_c,t_d. The amplitudes t_a and t_b represent hopping between nearest-neighbor oxygen sites, i.e., with $\omega(\Delta,\Delta')=1$, as in Fig. [2(a)]. We use t_a (t_b) for the case $\sigma=\uparrow$ ($\sigma=\downarrow$). Similarly, t_c and t_d represent hopping between next-nearest-neighbor oxygens, with $\omega(\Delta,\Delta')=0$, as in Fig. [2(b)]. From Eqs. (3.3), (3.4), (3.6), and (3.7) we thus find

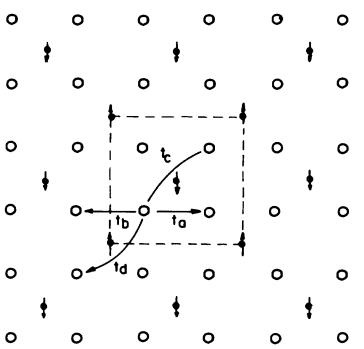

FIG. 3. Tight-binding amplitudes of the quasiparticle's hops.

$$
\begin{aligned}
t_a &= (t_1+t_0)(c_1^* c_1' + \tfrac{2}{3} c_2^* c_2' + \tfrac{1}{3} c_3^* c_3') \ , \\
t_b &= (t_1+t_0)(\tfrac{1}{3} c_2^* c_2' + \tfrac{2}{3} c_3^* c_3' + c_4^* c_4') \ , \\
t_c &= t_1(c_1^* c_1' + \tfrac{2}{3} c_2^* c_2' + \tfrac{1}{3} c_3^* c_3') \ , \\
t_d &= t_1(\tfrac{1}{3} c_2^* c_2' + \tfrac{2}{3} c_3^* c_3' + c_4^* c_4') \ ,
\end{aligned} \tag{3.8}
$$

for the spin-$\frac{3}{2}$ quasiparticle and

$$
\begin{aligned}
t_a &= (t_1+t_2)(-\tfrac{2}{3} d_1^* d_1' + \tfrac{1}{6} d_2^* d_2') \\
&\quad + (-t_2+t_0)(\tfrac{5}{6} d_1^* d_1' + \tfrac{1}{6} d_2^* d_2') \ , \\
t_b &= (t_1+t_2)(-\tfrac{2}{3} d_2^* d_2' + \tfrac{1}{6} d_1^* d_1') \\
&\quad + (-t_2+t_0)(\tfrac{5}{6} d_2^* d_2' + \tfrac{1}{6} d_1^* d_1') \ ,
\end{aligned} \tag{3.9}
$$

$$
t_c = (t_1+t_2)(-\tfrac{2}{3} d_1^* d_1' + \tfrac{1}{6} d_2^* d_2') - t_2(\tfrac{5}{6} d_1^* d_1' + \tfrac{1}{6} d_2^* d_2') \ ,
$$

$$
t_d = (t_1+t_2)(-\tfrac{2}{3} d_2^* d_2' + \tfrac{1}{6} d_1^* d_1') - t_2(\tfrac{5}{6} d_2^* d_2' + \tfrac{1}{6} d_1^* d_1') \ ,
$$

for the spin-$\frac{1}{2}$ quasiparticle.

We can check these results in an extreme limit. For $|\mathrm{qp}\rangle_5$ we find $t_b = t_d = 0$. Similarly, for $|\mathrm{qp}\rangle = |\downarrow\downarrow\downarrow\rangle$ we have $t_a = t_c = 0$. We notice that the quasiparticle $|\uparrow\uparrow\uparrow\rangle$ is localized around a spin-down Cu, whereas the quasiparticle $|\downarrow\downarrow\downarrow\rangle$ is localized around a spin-up Cu. Clearly, these quasiparticles cannot move without breaking the AFM order.

IV. THE BANDS

In this section we calculate the tight-binding bands. The wave function of the mobile quasiparticle ψ is periodic. Thus it can be written as

$$
\psi(\mathbf{r}) = \sum_{\mathbf{R}} e^{i\mathbf{k}\cdot\mathbf{R}} \phi(\mathbf{r}-\mathbf{R}) \ , \tag{4.1}
$$

where $\mathbf{R}$ is in the Bravais lattice and ϕ is the wave function in each unit cell. In our case,

$$
\phi(\mathbf{r}) = \sum_{n=1}^{4} b_n \Phi(\mathbf{r}-\mathbf{d}_n) \ , \tag{4.2}
$$

where

$$
\mathbf{d}_n = (0,0),(0,\tilde{a}),(\tilde{a},0)(\tilde{a},\tilde{a}) \ . \tag{4.3}
$$

Here, $\tilde{a} = a/\sqrt{2}$ is the nearest-neighbor distance between oxygens, where a is the distance between two Cu sites. $\mathbf{d}_n$ denotes the sites (1), (2), (3), and (4) in Fig. 1(b). As is well known,[33] the energy spectrum is obtained by solving the equations

$$
\varepsilon(\mathbf{k}) b_m = -\sum_n \left[\beta_{mn} + \sum_{\mathbf{R}} \gamma_{mn}(\mathbf{R}) e^{i\mathbf{k}\cdot\mathbf{R}} \right] b_n \ , \tag{4.4}
$$

where

$$
\beta_{mn} = -\int d\mathbf{r}\, \Delta U(\mathbf{r}) \Phi^*(\mathbf{r}-\mathbf{d}_m) \Phi(\mathbf{r}-\mathbf{d}_n) \tag{4.5}
$$

and

$$
\gamma_{mn}(\mathbf{R}) = -\int d\mathbf{r}\, \Delta U(\mathbf{r}) \Phi^*(\mathbf{r}-\mathbf{d}_m) \Phi(\mathbf{r}-\mathbf{d}_n-\mathbf{R}) \ . \tag{4.6}
$$

In our case,

$$
\beta_{12} = \beta_{21} = \beta_{13} = \beta_{31} = \beta_{34} = \beta_{43} = \beta_{24} = \beta_{42} = t_a \ , \tag{4.7a}
$$

$$
\beta_{14} = \beta_{41} = \beta_{23} = \beta_{32} = t_c \ . \tag{4.7b}
$$

For $\mathbf{R}_1 = (\pm 2\tilde{a}, 0)$, $\mathbf{R}_2 = (0, \pm 2\tilde{a})$, $\mathbf{R}_3 = (\pm 2\tilde{a}, \pm 2\tilde{a})$, and $\mathbf{R}_4 = (\pm 2\tilde{a}, \mp 2\tilde{a})$ we have

$$
\gamma_{12}(\mathbf{R}_1) = \gamma_{34}(\mathbf{R}_1) = \gamma_{21}(\mathbf{R}_1) = \gamma_{43}(\mathbf{R}_1) = t_b \ , \tag{4.8a}
$$

$$
\gamma_{13}(\mathbf{R}_2) = \gamma_{24}(\mathbf{R}_2) = \gamma_{31}(\mathbf{R}_2) = \gamma_{42}(\mathbf{R}_2) = t_b \ , \tag{4.8b}
$$

$$
\gamma_{41}(\mathbf{R}_3) = \gamma_{14}(\mathbf{R}_3) = t_d \ , \tag{4.8c}
$$

and

$$
\gamma_{23}(\mathbf{R}_4) = \gamma_{32}(\mathbf{R}_4) = t_d \ . \tag{4.8d}
$$

From now on we take the distance between two neighboring cells $2\tilde{a}$ as unity. Solving Eq. (4.4) amounts to finding the eigenvalues of the following 4×4 matrix,

$$
M = \begin{bmatrix}
0 & \alpha(\mathbf{k}) & \theta(\mathbf{k}) & \tilde{\delta}(\mathbf{k}) \\
\alpha^*(\mathbf{k}) & 0 & \delta(\mathbf{k}) & \theta(\mathbf{k}) \\
\theta^*(\mathbf{k}) & \delta^*(\mathbf{k}) & 0 & \alpha(\mathbf{k}) \\
\tilde{\delta}^*(\mathbf{k}) & \theta^*(\mathbf{k}) & \alpha^*(\mathbf{k}) & 0
\end{bmatrix} , \tag{4.9}
$$

where

$$
\begin{aligned}
&\alpha(\mathbf{k}) = t_a + B(\mathbf{k}) t_b, \quad \theta(\mathbf{k}) = t_a + C(\mathbf{k}) t_b \ , \\
&\delta(\mathbf{k}) = t_c + B(\mathbf{k}) C(\mathbf{k}) t_d, \quad \tilde{\delta}(\mathbf{k}) = t_c + B^*(\mathbf{k}) C(\mathbf{k}) t_d \ , \\
&B(\mathbf{k}) = e^{-ik_x}, \quad C(\mathbf{k}) = e^{-ik_y} \ .
\end{aligned} \tag{4.10}
$$

There are special points (Γ, L, and X) in the Brillouin zone, where $B(\mathbf{k})$ and $C(\mathbf{k})$ are real,

$$
\begin{aligned}
&\Gamma: \ B = C = 1 \ \text{ at } k_x = k_y = 0 \ , \\
&L: \ B = C = -1 \ \text{ at } k_x = k_y = \pm\pi \ , \\
&X: \ B = -C = 1 \ \text{ at } k_x = 0, \ k_y = \pm\pi \ , \\
&X: \ B = -C = -1 \ \text{ at } k_y = 0, \ k_x = \pm\pi \ .
\end{aligned}
$$

At these points we can find the eigenvalues analytically,

$$
\begin{aligned}
\varepsilon_1 &= 2t_a + (B+C) t_b + t_c + BC t_d \ , \\
\varepsilon_2 &= (B-C) t_b - t_c - BC t_d \ , \\
\varepsilon_3 &= (C-B) t_b - t_c - BC t_d \ , \\
\varepsilon_4 &= -2t_a - (B+C) t_b + t_c + BC t_d \ .
\end{aligned} \tag{4.11}
$$

Notice that the notation used above does not mean that the values of ε_i, for different values of B and C, should belong to the same band i. It is just the set of four energies at each specific point.

For other values of $\mathbf{k}$ we diagonalized M numerically, and the resulting four bands are presented in Fig. 4. The four parts of the figure were calculated for the four quasiparticles defined in Eqs. (2.5a), (2.5b), (2.6a), and (2.6d), using the parameters given after Eq. (3.1).

V. RESULTS

A. The best quasiparticle

The favored quasiparticle is the one for which the sum of exchange and kinetic energy is the lowest. From Fig. 4 we see that $|qp\rangle_1$ (and of course also the spin-reversed quasiparticle) has the lowest kinetic energy. Its minimum value is -3 eV. The minimum in the kinetic energy for the spin-$\frac{3}{2}$ quasiparticles is -0.8 eV. If $J_\sigma < 0$ then $|qp\rangle_1$ also has the lowest exchange energy and $|qp\rangle_1$ is favored. For $J_\sigma = -0.36$ eV (Ref. 29) the energy difference between the lowest energy of $|qp\rangle_1$ and the spin-$\frac{3}{2}$ quasiparticles amounts to ~ -2.8 eV. Since experimental and numerical results support the option of a negative J_σ we assume that indeed $|qp\rangle_1$ is the favored quasiparticle. If $J_\sigma > 0$, then J_σ should be greater than 1.5 eV in order to make the spin-$\frac{3}{2}$ quasiparticles favored. We would also like to add that the quasiparticle that can be formed by a superposition of $|\gamma_1\rangle$ and $|\gamma_2\rangle$, with zero exchange energy [mentioned after Eq. (2.4)], does not have a lower kinetic energy, and it is never favored.

The state $|qp\rangle_1$ is favored over $|qp\rangle_2$ by a small energy difference, of order 0.1 eV [compare Figs. 4(a) and 4(b)]. A classical calculation, which included the canting of all the Cu spins due to the frustration caused by the hole, indicated that the spin of the quasiparticle prefers to be or-

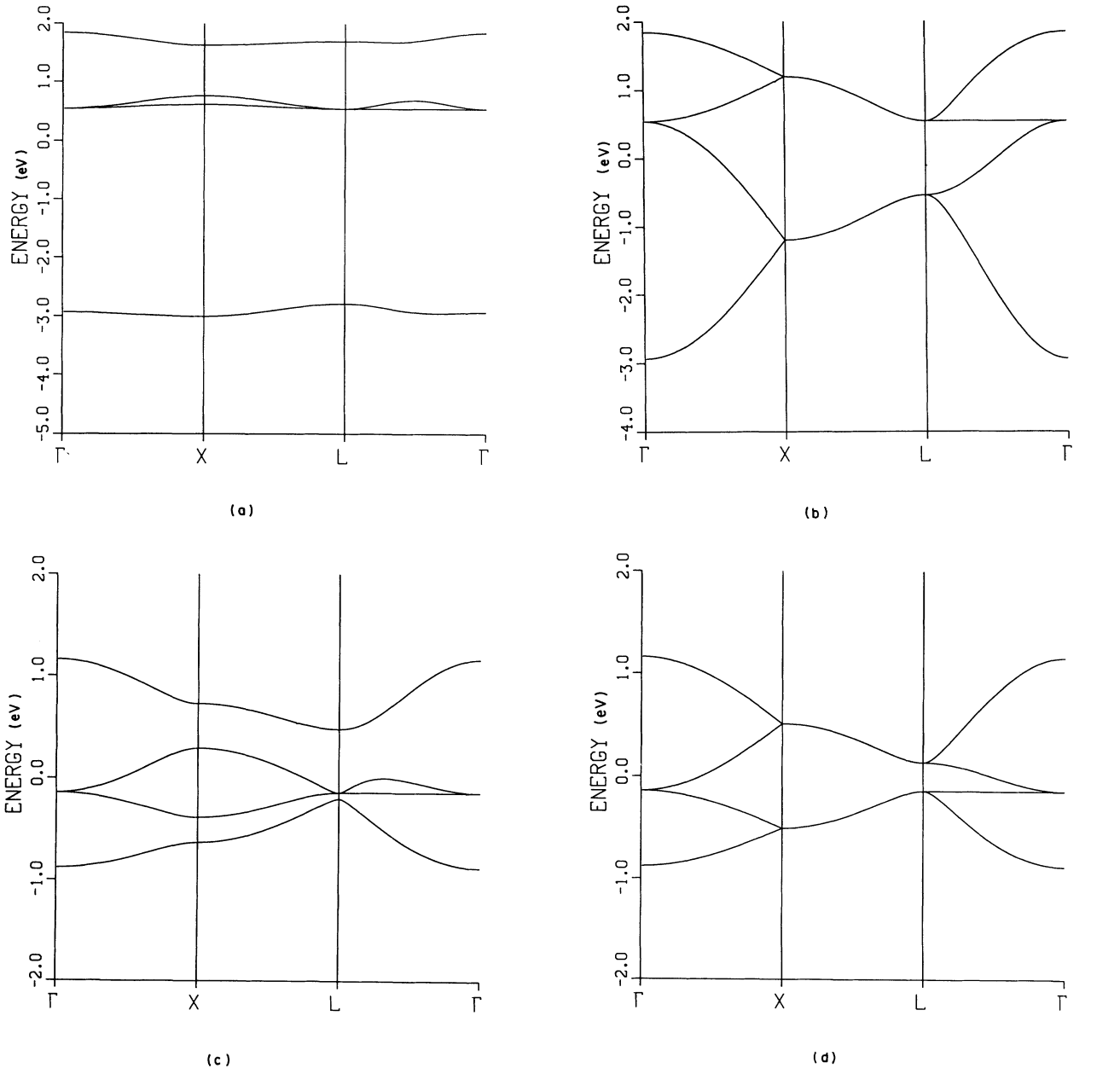

FIG. 4. Energy bands of the four studied quasiparticles: $|qp\rangle_1$, $|qp\rangle_2$, $|qp\rangle_3$, and $|qp\rangle_4$ in Figs. (a), (b), (c), and (d), respectively.

thogonal rather than parallel to the staggered magnetization in the planes,[12] and this would suggest that $|qp\rangle_2$ should be favored. Therefore, we carried out the calculations described below for this quasiparticle as well. The results for the phase diagram and for the effective mass are strongly inconsistent with the experimental data, and therefore this quasiparticle seems to be inappropriate. We cannot rule out the possibility that a state, whose spin is orthogonal to the staggered magnetization, would become favored if more Cu spins are included in the quasiparticle state.

The lowest band of the favored quasiparticle has its minimum at the points X, with $\mathbf{k}=(0,\pm\pi)$ or $\mathbf{k}=(\pm\pi,0)$. The band looks flat in comparison with the interband gap. Therefore, one might worry that the location of the minimum could be determined by small errors in the parameters. In order to check this possibility we notice that the lowest band corresponds to the values of ε_1 [Eq. (4.11)]. The minimum remains at X provided that

$$t_b+t_d>0 \ . \tag{5.1}$$

For this quasiparticle [see Eq. (3.9)]

$$t_b+t_d=\tfrac{1}{6}(t_0+2t_1) \ , \tag{5.2}$$

thus the condition is

$$t_0+2t_1>0 \ . \tag{5.3}$$

For our choice of parameters,

$$t_0+2t_1=0.21 \text{ eV} \ . \tag{5.4}$$

Therefore a small change in the choice of parameters cannot change this result. Actually, Eq. (5.3) holds for all the values presented in Table I. However, it would help to reduce the scatter in the values of the parameters that is manifested in this table.

B. Density of states

The density of states of the lowest energy band was evaluated by diagonalizing the matrix M [Eq. (4.9)] for a dense grid of points in the Brillouin zone. Since we are interested in the properties of our system as a function of doping, we present in Fig. 5 the density of states as a function of the doping concentration x. We see that the maximum density of states is obtained at $x\simeq 0.45$ and that the density of states is very low for $x\geq 0.65$. In the second paper in this series[34] we shall use the density of states and the BCS equation[35] to calculate the superconductivity phase diagram.

C. Effective mass and penetration depth

We next calculate the in-plane effective mass of the best quasiparticle. We first expand the eigenvalue ε_1 near the extremum ε_1 [Eq. (4.11)], in a perturbation series in the deviations Δk_x and Δk_y

$$\varepsilon_1(\Delta\mathbf{k})=\varepsilon_1(0)+\left[\frac{(t_bB+t_dBC)^2}{2(t_a+Bt_b+t_c+BCt_d)}-\tfrac{1}{2}(Bt_b+BCt_d)\right]\Delta k_x^2+\left[\frac{(t_bC+t_dBC)^2}{2(t_a+Ct_b+t_c+BCt_d)}-\tfrac{1}{2}(Ct_b+BCt_d)\right]\Delta k_y^2$$
$$=e_{xx}\Delta k_x^2+e_{yy}\Delta k_y^2 \ . \tag{5.5}$$

For the best quasiparticle, the minimum occurs at the point X, i.e., $B=-C=\pm 1$. We next write,

$$e_{\alpha\alpha}=\frac{\hbar^2}{2m_{\alpha\alpha}} \ . \tag{5.6}$$

Since in our case we took the length $2\bar{a}=a\sqrt{2}$ (a being the Cu-Cu distance) as unity we should divide $m_{\alpha\alpha}$ by $2a^2$ and $a^2\simeq 1.4\times 10^{-19}m$. Measuring $e_{\alpha\alpha}$ in units of eV we end up with

$$\frac{m_{\alpha\alpha}}{m_e}=\frac{0.13}{e_{\alpha\alpha}} \ . \tag{5.7}$$

For the parameters $t_0=-0.65$ eV, $t_1=0.43$ eV, and $t_2=0.22$ eV, we substitute for $|qp\rangle_1$ $d_1=1$ and $d_2=0$ in Eq. (3.9) and obtain $t_a=-1.16$ eV, $t_b=-0.04$ eV, $t_c=-0.62$ eV, and $t_d=0.72$ eV. We use these values in Eq. (5.9) to obtain $e_{\alpha\alpha}=0.051$ eV or 0.017 eV. Thus, near $\mathbf{k}=(\pm\pi,0)$, $m_{xx}=2.5m_e$ and $m_{yy}=7.5m_e$, whereas near $\mathbf{k}=(0,\pm\pi)$, $m_{yy}=2.5m_e$ and $m_{xx}=7.5m_e$.

The effective mass, obtained by averaging the derivatives of the energy over all four X points, is

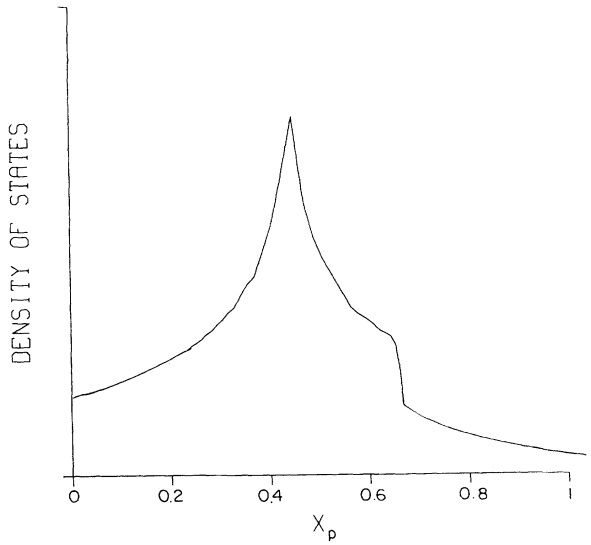

FIG. 5. Density of states of the lowest-energy band as a function of doping.

TABLE II. Comparison of the estimated concentration of holes in the CuO_2 planes x_p by inserting the measured in-plane penetration depths λ, the volume of the unit cell V, and the number of CuO_2 planes per unit cell l.

Compound	T_c K	λ Å	V Å (Ref. 3)	l	x_p
$Bi_2(Sr,Ca)_2CuO_{8+\delta}$	84 (Ref. 45)	3500 (Ref. 45)	714 (Ref. 45)	4	0.15
$Bi_2CaSr_2Cu_2O_8$	82 (Ref. 46)	1950 (Ref. 46)	453 (Ref. 47)	4	0.31
$Tl_2Ca_2Ba_2Cu_3O_{10}$	105 (Ref. 46)	1850 (Ref. 46)	529 (Ref. 48)	6	0.27
$YBa_2Cu_3O_7$	90 (Ref. 49)	1300–1470 (Ref. 49)	174 (Ref. 50)	2	0.42–0.54

$$m^* \simeq 3.7 m_e \ . \tag{5.8}$$

We may compare this value with $m^* \simeq 3.2 m_e$, which Tanaka *et al.*[36] estimated from optical spectra in the La compound or with $m^* \simeq 4 m_e$, which Krusin-Elbaum *et al.*[37] estimated for the $YBa_2Cu_3O_{6+y}$ compound. In our calculations we disregarded hops that disturb the AFM order. This limitation may increase the effective mass of these quasiparticles, which means that we should regard Eq. (5.8) as an upper limit.

The penetration depth in the planes λ is given by the London Equation,[38]

$$\lambda = \left[\frac{m^* c^2}{4\pi n e^2} \right]^{0.5} \ . \tag{5.9}$$

Using our estimate for m^*, this yields

$$\lambda \simeq 102 \sqrt{V/l x_p} \ \text{Å} \ , \tag{5.10}$$

where $V = a \times b \times c$ is the volume of the unit cell in Å^3 (a and b are the nearest-neighbors distances between Cu's in the CuO_2 plane), l is the number of CuO_2 planes per unit cell, and x_p is the number of holes in the CuO_2 planes per Cu in these planes. For $La_{2-x}Sr_xCuO_4$ the lattice constants are $a \simeq b \simeq 3.80$Å and $c \simeq 13.17$ Å.[39] Therefore,

$$\lambda_{La} \simeq \frac{1010}{\sqrt{x}} \ \text{Å} \ . \tag{5.11}$$

Grebinnik *et al.*[40] measured λ_{La} for $x = 0.1$ and $x = 0.15$, and obtained (3200±70 Å) and (2420±70 Å), respectively. These experimental results may be compared with $\simeq$3190 Å and $\simeq$2600 Å, obtained from Eq. (5.11). This agreement is quite encouraging.

For the other HTSC the comparison is more difficult, since we usually do not have for the same sample data on the concentration of holes and on the penetration depth. However, the measured phase diagrams for $La_{2-x}Sr_xCuO_4$,[41] $YBa_2Cu_3O_{6+y}$,[42] and $Bi_2Sr_2CaCu_2O_{8+\delta}$,[43] where T_c is measured as a function of the concentration of holes in the CuO_2 planes, indicate that high-temperature superconductivity is obtained only in the range $0.1 \le x_p \le 0.3$. Therefore, we insert the data on the penetration depth in Eq. (5.10) in order to estimate the concentration of holes and then check its consistency with the measured phase diagrams. In Table II we present the estimated concentrations based on the data of the penetration depths. We find consistent results for Bi and Tl compounds. For $YBa_2Cu_3O_7$ we find $x_p \simeq 0.54$ and this is inconsistent with the measured phase diagram and also with direct measurements of the concentration of holes in the CuO_2 planes.[42,44] A possible explanation for this discrepancy could be a different effective mass. However, there is no clear reason why the effective mass fits the other compounds and does not fit $YBaCu_3O_7$. Moreover, as mentioned before, independent experimental evidences[37] indicate that this is indeed the approximate value of the effective mass in $YBa_2Cu_3O_7$. It is possible that not only the CuO_2 planes superconduct but also the CuO chains. This suggestion is supported by the two recent reports, one by Welp *et al.*[51] who observed metallic behavior of the CuO chains in resistivity measurements of a single and untwinned $YBa_2Cu_3O_7$ crystal in its normal state and the second report was by Loram *et al.*[52] who concluded that there is a chain superconductivity from specific heat measurements of $YBa_2(Cu_{1-x}Co_x)_3O_{7-\delta}$.

VI. SUMMARY AND DISCUSSION

We studied a tight-binding model for the doped CuO_2 planes, which are a common ingredient in many HTSC. We took into account the influence of the AFM correlations of the Cu's spins on the oxygen doped holes, thus obtaining a four-band model for the doped holes. The spin of the doped hole strongly couples with the spins of the two neighboring Cu's. We therefore considered eigenstates of this interaction as possible quasiparticles.

We calculated hopping integrals for various quasiparticles. For simplicity we neglected disturbances of the AFM background due to hoppings. We found that the spin-$\frac{1}{2}$ quasiparticle is favored and that its effective mass is bounded from above by $3.7 m_e$.

We checked our estimate for the effective mass by evaluating the London penetration depth. We found encouraging agreement with experimental data for $La_{2-x}Sr_xCuO_4$. We also found that the penetration depths in Bi and Tl compounds are consistent with our estimates. However, the penetration depth of $YBa_2Cu_3O_7$ is totally inconsistent. A plausible explanation for this discrepancy may be that in the CuO chains also superconduct.

In the next paper in this series we will study the superconductivity phase diagrams, and we will discuss the main factors that determine their shapes.

ACKNOWLEDGMENTS

We thank R. J. Birgeneau, M. A. Kastner, V. J. Emery, G. Reiter, A. B. Harris, O. Entin-Wohlman, and U. Dai for many useful discussions. This work was supported in parts by grants from the U.S.-Israel Binational Science Foundation and from IBM.

[1]J. G. Bednorz and K. A. Müller, Z. Phys. B **64**, 189 (1986).
[2]M. K. Wu, J. R. Ashburn, C. J. Torng, P. H. Hor, R. L. Meng, L. Gao, Z. J. Huang, Y. Z. Wang, and C. W. Chu, Phys. Rev. Lett. **58**, 908 (1987).
[3]C. C. Torardi, M. A. Subramanian, J. C. Calabresa, J. Gopalakrishnan, E. M. McCarron, K. J. Morrissey, T. R. Askew, R. B. Flippen, U. Chowdhry, and A. W. Sleight, Phys. Rev. B **38**, 225 (1988).
[4]N. W. Preyer, R. J. Birgeneau, C. Y. Chen, D. R. Gabbe, H. P. Jenssen, M. A. Kastner, P. J. Picone, and T. Thio, Phys. Rev. B **39**, 11 563 (1989).
[5]N. Nücker, H. Romberg, S. Nakai, B. Scheerer, J. Fink, Y. F. Yan, and Z. X. Zhao, Phys. Rev. B **39**, 12 379 (1989).
[6]P. Steiner, S. Hüfner, V. Kinsinger, I. Sander, B. Siegwarth, H. Schmitt, R. Schulz, S. Junk, G. Schwitzgebel, A. Gold, C. Politis, H. P. Müller, R. Hoppe, S. Kemmler-Sack, and C. Kunz, Z. Phys. B **69**, 449 (1988).
[7]J. A. Yarmoff, D. R. Clarke, W. Drube, U. O. Karlsson, A. Taleb-Ibrahimi, and F. J. Himpsel, Phys. Rev. B **36**, 3967 (1987).
[8]M. Takigawa, P. C. Hammel, R. H. Heffner, and Z. Fisk, Phys. Rev. B **39**, 7371 (1989).
[9]Y. Guo, J. M. Langlois, and W. A. Goddard III, Science **239**, 896 (1988).
[10]A. K. Mcmahan, R. M. Martin, and S. Satpathy, Phys. Rev. B **38**, 6650 (1988).
[11]D. Vaknin, S. K. Sinha, D. E. Moncton, D. C. Johnston, J. M. Newsam, C. R. Safinya, and H. E. King, Jr., Phys. Rev. Lett. **58**, 2802 (1987); K. Yamada, E. Kudo, Y. Endoh, Y. Hidaka, M. Oda, M. Suzuki, and T. Murakami, Solid State Commun. **64**, 753 (1987).
[12]A. Aharony, R. J. Birgeneau, A. Coniglio, M. A. Kastner, and H. E. Stanley, Phys. Rev. Lett. **60**, 1330 (1988); A. Aharony, R. J. Birgeneau, and M. A. Kastner, IBM J. Res. Dev. **33**, 287 (1989); R. J. Birgeneau, M. A. Kastner, and A. Aharony, Z. Phys. B **71**, 57 (1988).
[13]Y. Kitaoka, K. Ishida, T. Kobayashi, K. Amaya, and K. Asayama, Physica C **153**, 733 (1988).
[14]J. L. Budnick, B. Chamberland, D. P. Yang, Ch. Niedermayer, A. Golnik, E. Recknagel, M. Rossmanith, and A. Weidinger, Europhys. Lett. **5**, 651 (1988).
[15]K. Kumagai, I. Watanabe, H. Aoki, Y. Nakamura, T. Kimura, Y. Nakamichi, and H. Nakajima, Physica B **148**, 480 (1987).
[16]D. W. Harshman, G. Aeppli, G. P. Espinosa, A. S. Cooper, J. P. Remeika, E. J. Ansaldo, T. M. Riseman, D. Ll. Williams, D. R. Noakes, B. Ellman, and T. F. Rosenbaum, Phys. Rev. B **38**, 852 (1988).
[17]R. J. Birgeneau, D. R. Gabbe, H. P. Jenssen, M. A. Kastner, P. J. Picone, T. R. Thurston, G. Shirane, Y. Endoh, M. Sato, K. Yamada, Y. Hidaka, M. Oda, Y. Enomoto, M. Suzuki, and T. Murakami, Phys. Rev. B **38**, 6614 (1988).
[18]A. Rigamonti, F. Borsa, M. Corti, T. Rega, J. Ziola, and F. Waldner, in *Earlier and Recent Aspects of Superconductivity,* Springer Series in Solid-State Science, Vol. 90, edited by J. G. Bednorz and K. A. Müller (Springer-Verlag, Berlin, 1990), p. 441.
[19]P. Fulde and G. Zwiknagl, in *Earlier and Recent Aspects of Superconductivity,* Springer Series in Solid-State Science Vol. 90, edited by J. G. Bednorz and K. A. Müller (Springer-Verlag, Berlin, 1990), p. 326.
[20]M. Frick and T. Schneider, Z. Phys. B **78**, 159 (1990).
[21]F. C. Zhang and T. M. Rice, Phys. Rev. B **37**, 3759 (1988).
[22]V. J. Emery, Phys. Rev. Lett. **58**, 2794 (1987).
[23]B. I. Shraiman and E. D. Siggia, Phys. Rev. Lett. **61**, 467 (1988).
[24]O. Entin-Wohlman and Y. Imry, Phys. Rev. B **40**, 6731 (1989).
[25]V. J. Emery and G. Reiter, Phys. Rev. B **38**, 4547 (1988).
[26]M. S. Hybertsen, M. Schlüter, and N. E. Christensen, Phys. Rev. B **39**, 9028 (1989).
[27]E. B. Stechel and D. R. Jennison, Phys. Rev. B **38**, 4632 (1988).
[28]H. Eskes, G. A. Sawatzky, and L. F. Feiner, Physica C **160**, 424 (1989); G. A. Sawatzky, in *Earlier and Recent Aspects of Superconductivity,* Springer Series in Solid-State Science, Vol. 90, edited by J. G. Bednorz and K. A. Müller (Springer-Verlag, Berlin, 1990), p. 345.
[29]D. M. Frenkel, R. J. Gooding, B. I. Shraiman, and E. D. Siggia, Phys. Rev. B **41**, 350 (1990).
[30]M. Ogata and H. Shiba, J. Phys. Soc. Jpn. **57**, 3074 (1988).
[31]J. R. Schrieffer, X. G. Wen, and S. C. Zhang, Phys. Rev. Lett. **60**, 944 (1988).
[32]J. Fink, J. P. Pflüger, Th. Müller-Heinzerling, N. Nücker, B. Scheerer, H. Romberg, M. Alexander, R. Manzke, T. Buslaps, and R. Claessen, in *Earlier and Recent Aspects of Superconductivity,* Springer Series in Solid-State Science, Vol. 90, edited by J. G. Bednorz and K. A. Müller (Springer-Verlag, Berlin, 1990), p. 377.
[33]N. W. Ashcroft and N. D. Mermin, *Solid State Physics* (Holt, Rinehart and Winston, New York, 1976), Chap. 10.
[34]L. Klein and A. Aharony (unpublished).
[35]J. Bardeen, L. N. Cooper, and J. R. Schrieffer, Phys. Rev. **108**, 1175 (1957).
[36]J. Tanaka, M. Shimada, U. Mizutani, and M. Hasegawa, Physica C **153**, 651 (1988).
[37]L. Krusin-Elbaum, R. L. Greene, F. Holtzberg, A. P. Malozemoff, and Y. Yeshurun, Phys. Rev. Lett. **62**, 217 (1989).
[38]F. London and H. London, Proc. R. Soc. London, Ser. A **149**, 71 (1935).
[39]M. A. Subramanian, C. C. Torardi, J. Gopalakrishnan, J. C. Calabresa, K. J. Morrissey, T. R. Askew, R. B. Flippen, U. Chowdhry, A. W. Sleight, J. J. Lin, and S. J. Poon, Physica C **153**, 608 (1988).
[40]V. G. Grebinnik, V. N. Duginov, V. A. Zhukov, S. Kapusta, A. B. Lazarev, V. G. Olshevsky, V. Yu. Pomjakushin, S. N. Shilov, I. I. Gurevich, B. F. Kirillov, B. A. Nikolsky, A. V. Pirogov, A. N. Ponomarev, V. A. Suetin, I. V. Kurachatov, A. G. Peresada, M. D. Nersesyan, I. P. Borovinskaya, V. R. Karasik, O. E. Omelyanovsky, and T. G. Togonidze, Physica C **162**, 145 (1989).
[41]J. B. Torrance, Y. Tokura, A. Nazzal, A. Bezinge, T. C. Huang, and S. S. P. Parkin, Phys. Rev. Lett. **61**, 1127 (1988).
[42]Y. Tokura, J. B. Torrance, T. C. Huang, and A. I. Nazzal, Phys. Rev. B **38**, 7156 (1988).
[43]W. A. Groen, D. M. de Leeuw, and L. F. Feiner, Physica C **165**, 55 (1990); Y. Koike, Y. Iwabuchi, S. Hosoya, N. Kobayashi, and T. Fukase, *ibid.* **159**, 105 (1989).
[44]Z. Z. Wang, J. Clayhold, N. P. Ong, J. M. Tarascon, L. H. Greene, W. R. McKinnon, and G. W. Hull, Phys. Rev. B **36**, 7222 (1987).
[45]P. Birrer, F. N. Gygax, B. Hettich, B. Hitti, E. Lippelt, H. Maletta, A. Schenck, and M. Weber, Physica C **158**, 230 (1989).
[46]R. L. Lichti, K. C. B. Chan, D. W. Cooke, and C. Boekema, Appl. Phys. Lett. **54**, 2361 (1989).
[47]S. A. Sunshine, T. Siegrist, L. F. Schneemeyer, D. W. Murphy, R. J. Cava, B. Batlogg, R. B. Van Dover, R. M. Fleming,

S. H. Glarum, S. Nakahara, R. Farrow, J. J. Krajewski, S. M. Zahurak, J. V. Waszczak, J. H. Marshall, P. Marsh, L. W. Rupp, Jr., and W. F. Peck, Phys. Rev. B **38**, 893 (1988).

[48]B. Morosin, D. S. Ginley, J. E. Schirber, and E. L. Venturini, Physica C **156**, 587 (1988).

[49]B. Pümpin, H. Keller, W. Kündig, W. Odermatt, I. M. Savic, J. W. Schneider, H. Simmler, P. Zimmermann, J. G. Bednorz, Y. Maeno, K. A. Müller, C. Rossel, E. Kaldis, S. Rusiecki, W. Assmus, and J. Kowalewski, Physica C **162-164**, 151 (1989); Y. J. Uemura, V. J. Emery, A. R. Moodenbaugh, M. Suenaga, D. C. Johnston, A. J. Jacobson, T. Lewandowski, J. H. Brewer, R. F. Kiefl, S. R. Kreitzman, G. M. Luke, T. Riseman, C. E. Stronach, W. J. Kossler, J. R. Kempton, X. H. Yu, D. Opie, and H. E. Schone, Phys. Rev. B **38**, 909 (1988); D. R. Harshman, L. F. Schneemeyer, J. V. Waszczak, G. Aeppli, R. J. Cava, B. Batlogg, L. W. Rupp, E. J. Ansaldo, and D. Ll. Williams, *ibid.* **39**, 851 (1989).

[50]R. Calemczuk, E. Bonjour, J. Y. Henry, L. Forro, C. Ayache, M. J. M. Jurgens, J. Rossat-Mignod, B. Barbara, P. Burlet, M. Couach, A. F. Khoder, and B. Salce, Physica C **153-155**, 960 (1988); M. Francois, A. Jonod, K. Yvon, P. Fischer, J. J. Capponi, P. Strobel, and M. Marezio, *ibid.* **153-155**, 962 (1988).

[51]U. Welp, S. Fleshler, W. K. Kwok, J. Downey, Y. Fang, G. W. Crabtree, and J. Z. Liu, Supercond. Sci. Technol. **4**, S409 (1991).

[52]J. W. Loram, K. A. Mirza, P. F. Freeman, and J. J. Tallon, Supercond. Sci. Tehcnol. **4**, S184 (1991).